Production and Characterization of Antibacterial Effective Nanofiber from TPU-Ag NPs and PLA Designed using Coaxial Electrospinning for Potential Use in Wound Dressing

Sema, Samatya Yilmaz
Polymer Science and Technology Department, Kocaeli University, Kocaeli, TURKEY

Aytac, Ayse*[*+•]*
Polymer Science and Technology Department, Kocaeli University, Kocaeli, TURKEY

ABSTRACT: *In this study, a novel bicomponent nanomaterial has been designed to be used as an antibacterial effective wound dressing for dry wounds. These nanofibers' wound dressing successfully have been produced by coaxial electrospinning method feeding neat polylactic acid into the core and thermoplastic polyurethane-silver nanoparticles into the shell. In addition to examining the antibacterial and cytotoxicity properties of the designed polymeric nanomaterials, physical and chemical characterization studies have been also carried out. It has been determined that the 10% silver nanoparticles doped bicomponent nanomaterial had the thinnest smooth nanofibers with 1127 nm value, the highest hydrophobic behavior with 131° contact angle value, the highest tensile strength with 2.53 MPa value, and the highest flexibility with 66.84% value. In addition, 10% and 5% silver nanoparticles doped bicomponent nanofibers have been indicated to have high cell viability with values of about 90% and 80% respectively. It has been emphasized that these bicomponent electrospun mats, which have been improved for dry wounds can be used as a 100% antibacterial effective wound dressing against Escherichia coli, staphylococcus aureus, and Pseudomonas aeruginosa if it is renewed every 24 hours.*

KEYWORDS: *Antibacterial, Bicomponent Nanofiber; Coaxial Electrospinning; Dry Wounds, PLA/TPU-AgNP Wound Dressing.*

INTRODUCTION

In recent years, there has been an increasing interest in using biodegradable, non-petroleum-based, and sustainable resources. Especially nano-scale or micro-scale materials of natural origin exhibit high mechanical strength and

**To whom correspondence should be addressed.*
+ E-mail: aaytac@kocaeli.edu.tr
• Other Address: Chemical Engineering Department, Kocaeli University, Kocaeli, TURKEY
1021-9986/2023/9/2857-2875 18/$/6.08

flexibility [1]. The coaxial electrospinning method displayed enormous prospects to discover the following generation of polymers by fabricating excellent nanoscale structures while saving the individual properties of the bicomponent materials [2]. One or more of the components used in this method should have a cross-section in the nano-scale to fabricate electrospun mats. This bicomponent electrospinning process may be used for the production of minor diameter electrospun mats as well as to create multi-component electrospun mats. The cross-section shapes of the often-produced bicomponent nanofibers are core-shell, side-by-side, islands-in-the-sea, segmented-pie, segmented-ribbon, and hollow segmented pie. Core-shell bicomponent nanofiber production is carried out by coaxial electrospinning, using the spinneret with a coaxial nozzle where an outer polymer solution (shell) and an inner polymer solution (core). In this process, two syringe pumps are used to feed the polymer solutions independently. When electrostatic repulsions between surface charges are overcome, the shell polymer solution of the combined droplets stretches, and thus, viscous stress forms. Next, it is transferred to the core of the nanofiber, and the core polymer solution is rapidly elongated. Thereby, the combined jet is obtained, producing coaxial nanofibers. Bicomponent nanofibers begin to accumulate on the collector plate [3]. To develop the mechanical performances of polymeric materials, some polymers are used by blending with suitable polymers or in the form of single a composite structure (without mixing) in combination with other polymers [4]. Although poly(lactic) acid (PLA) is brittle and has weak mechanical properties, it is frequently used in biomedical applications because it is a biodegradable and biocompatible material [5]. The production and use of naturally sourced biomaterials are preferred in tissue engineering. These materials, which support cell attachment and proliferation, can also carry biodegradability [6]. Thermoplastic polyurethane (TPU) also, which has high elasticity and strong mechanical properties, is partially compatible with blood [7]. Mechanical properties are improved when PLA and TPU structures are used together [8]. The nanofibers produced from PLA [9] and TPU [10] are suitable for the fabrication of the tissue scaffold for they satisfy wound dressing properties. Even, due to their natural structure, nano/micro electrospun mats meet the requirements for wound dressing owing to many superior features like high porosity, air permeability, and large surface area/volume ratio [11]. To fabricate an antibacterial effective wound dressing the studies of adding into the polymer matrix of particularly silver nanoparticles (Ag-NPs or n-Ag) among nano-sized metals have increased considerably in recent years [12]. Because silver has high antibacterial properties due to its nature. It has been used since ancient times to destroy viruses and bacterium types such as gram-positive or gram-negative. It is preferred safely in the production of wound dressings due to its non-toxic effect and its ability to inhibit the respiratory systems of harmful structures [13].

In our previous study, poly(lactic) acid and polyurethane mixed nanofibers were obtained with a simple electrospinning method, and their characterization properties were examined [8]. In contrast, in this study, a single two-component nanomaterial was produced from PLA and TPU polymers by coaxial electrospinning method without mixing. A completely new bicomponent nanomaterial was obtained with the changing production method and its characterization properties were investigated. Although there are no studies on the production of bicomponent electrospun mats from PLA and TPU polymers in the literature, there also are no studies on the design of antibacterial effective wound dressings with Ag NP additives. Different from this study, investigations on nanofiber applications in the literature, which were studied with Ag-doped TPU and PLA, are summarized.

Nguyen et al fabricated biodegradable nanofibers of core PLA and Chitosan Shell (CS) with coaxial electrospinning for biomedical applications [14]. *Hajikhani et al* used the PLA/Poly (ethylene oxide) (PEO) blend as the core and the polyvinylpyrrolidone (PVP) as the shell. The nanomaterial having high mechanical properties, biodegradable and biocompatible has been obtained [15]. *Lakshman et al* investigated the antibacterial properties, cytotoxicity features, and water absorption of the PU-Ag nanofiber and compared the wound dressing structures used today with PU foam. It has been displayed that the PU-Ag nano-webs may be used for wound dressing applications [13]. In the study of *Zeytuncu* and *Morcali*, the Ag NPs have been added to the polyurethane polymer matrix with the photocured process. The photocured materials containing Ag NPs displayed high antibacterial efficiency against *S. aureus* and *E. coli* [16].

Table 1: The study codes of all bicomponent nanofibers

Study Codes	AgNPs (wt%)	Core	Shell	Concentration of Solution (wt%)	Structure of Nanofibers
Neat PLA	-	-	-	10	single
Neat TPU	-	-	-	10	single
coPLAshTPU	-	Neat PLA	Neat TPU	-	bicomponent
coPLAsh2AgTPU	2	Neat PLA	TPU-Ag NP blend	10	bicomponent
coPLAsh5AgTPU	5				
coPLAsh10AgTPU	10				

Hsu et al, the various low concentrations of Ag NPs have been doped to waterborne-based polyester-type polyurethane (PU) matrix in their study. The high biocompatibility of the TPU/Ag NP nanomaterial films was examined for rat hypodermic. Nanostructures demonstrated antibacterial activity against *E.coli*. PU/Ag NP nanocomposites are suggested as a potential cardiovascular biomaterial [17].

In this study, when PLA and TPU are used together without mixing, preserving their specific properties, it was planned to obtain bicomponent nanofibers with improved mechanical properties and higher hydrophobic character. Therefore, a highly antibacterial effective bicomponent nanofiber wound dressing production was designed for dry wounds. For TPU/Ag NPs and neat PLA, the layout design in bicomponent structure has been made with some critical points in mind. It was considered that the designed bicomponent nanofibers should have a certain cell viability value to be used as a wound dressing. For this purpose, it has been aimed that when neat PLA forms the inner core, the biodegradable and high biocompatibility properties appear, and when PU-Ag NP forms the outer shell, higher antibacterial properties together with superior mechanical properties (thus free patient movements) occur. It has been thought that these nanomaterials obtained with coaxial electrospinning by using AgNPs in the outer shell will provide high antibacterial activity on the skin tissue area it comes into contact with. In addition, it was foreseen that the presence of Ag NPs used in the shell would support the higher hydrophobic character structure, and thus can easily be used for dry wounds, and the layout was provided accordingly. Antibacterial and cytotoxicity tests of the obtained PLA/PU Ag NPs bicomponent nanofiber wound dressings were performed. Moreover, their characterization was defined by analyses of morphological, chemical, thermal, surface wettability, and mechanical properties. All results have been reported as elaborate.

EXPERIMENTAL SECTION

Materials

4043D Poly (lactic) acid (PLA) was purchased from Nature Works. The aromatic polyether-based Thermoplastic Polyurethane (TPU) named Estane®GP52DTNAT055 was supplied by Lubrizol (Velox). Dimethylformamide (DMF) and chloroform (CF) which solvents used in this study were assured by Merck Company. The silver nanoparticles (Ag NPs) that have 35 nm size and 99,99% purity were purchased from Nanografi.

Preparation of bicomponent electrospun nonwovens

Firstly, the PLA and the TPU granules waited for 12 h in the oven at 80°C. So, the moisture in the granules was cleared up. The 10 wt% neat PLA solution, the 10 wt% neat TPU solution, and the 10 wt% TPU/Ag NP solutions were prepared in the blending solvent CF/DMF (8/2, v/v) with magnetic stirring for 3h at room temperature. At the end of 3 hours, the 10 wt.% pure TPU solution temperature and the 10 wt.% TPU/Ag NP solutions were raised to 120ºC temperature, and the stirring was continued for 30 min. Thus, all solutions were obtained as homogeneous and fully dissolved.

The electrospinning device that has a high-voltage DC instrument with a practical voltage of max 30 kV, to the two feeding pumps and the aluminum collector plate, was provided by Inovenso Company. Formed all solutions were used in the electrospinning process without waiting. The study codes obtained for all electrospun mats are shown in Table 1.

Initially, the neat PLA and the neat TPU nanofibers were produced as control samples. These nanofibers were obtained with conditions of 0.5 mL/h feeding speed, 20 cm distance, and 15 kV supplied voltage by using the 22G needle-tipped syringe in the single electrospinning process. Di-axial electrospinning operation parameters were determined

as 1.00 mL/h feeding rate, 21 kV applied voltage, and 23 cm distance between syringe and collector. The spinning conditions mentioned are results optimized with many experimental studies. Since it is known that different production conditions will have different effects on fiber properties, process conditions were kept constant for all bicomponent fibers. In the bicomponent electrospinning process, was used a di-axial needle that has an inner diameter of 0.64 mm (22G) and an outer diameter of 1.6 mm (14G). Also, the electrospinning process was achieved at 24ºC (±2) and relative humidity of 65% (±3). The conductivity value of the CF/DMF (8/2, v/v) solvent blend at room temperature (24°C) was measured as 0.3 µS/cm at 24ºC (±2) with a Mettler Toledo branded liquid conductivity meter.

Characterization

The microscopic morphology and fiber diameter distribution of the electrospun mats were examined with QUANTA 400F Field Emission branded Scanning Electron Microscopy (SEM). To obtain clear surface images by providing high transmittance in SEM analysis, the samples were coated with Au-Pd at a thickness of 3 mm before imaging. In addition, Energy Dispersive X-Ray Analysis (EDX) has been performed along with SEM analysis. With SEM-EDX, the distribution of Ag elements in the structure of nanofibers has been determined quantitatively.

FEI 120kV HCTEM branded Transmission Electron Microscope (TEM) was used to view the fiber surface structure in the inner core and outer shell, and to measure the inner core fiber diameter and Ag NP diameter. TEM samples were prepared by us. A copper grid with a diameter of 3 mm (the grid with a lot of pores) was attached to the collector plate with a band-aid. The bicomponent electrospinning process has been started, the process has been stopped after 30 seconds and the grid has been carefully removed from the collector plate and sent for analysis.

Flow times of neat solvents and solvent blends were measured for the relative viscosity determination. Then, 1% concentration solutions of neat TPU, neat PLA, and TPU-Ag NP blend solutions were prepared. Flow time measurement of each solution was realized with Koehler branded Ubbelohde at 24ºC (±2). The ratio of relative viscosity (η_r) of neat TPU, neat PLA, and TPU-Ag NP blend solutions were calculated from the flow time measurement with the following Equation (1):

$$\eta_r = \frac{\eta}{\eta_0} = \frac{t}{t_0} \quad (1)$$

Where η is the viscosity of the solution, η_0 is the solvent viscosity, ηr is the relative viscosity, t is the flow time of the solution, and t_0 is solvent flow time.

The chemical structure analysis that belongs to IR spectra in the range of 650-4000 cm^{-1} was defined by using a Perkin Elmer Spectrum 100 FTIR device with ATR unit spectrometric.

The thermogravimetric analysis of the nonwoven nanofibers was realized with a Mettler Toledo TGA 1 device in the range of 25°C to 600°C, with a heating rate of 10°C/min. differential scanning calorimetry (DSC) analysis was realized by using the Mettler Toledo DSC 1 device and DSC analysis of electrospun bicomponent mats was performed in a single-stage running the temperature range (-50°C) and 300°C with a heating speed of 10°C/min., The high-purity nitrogen gas to the system was sent at a flow speed of 50 mL/min during the analysis of the thermal properties of both TGA and DSC.

Wettability features of bicomponent electrospun mats were examined by dropping 10µl distilled water onto the surface with the Attension Theta Lite device at room temperature (24˚C ± 2˚C) thanks to the static contact angle measurement. The distilled water droplet was viewed on the computer through a camera that had an influential optical lens. The γ value of the droplet contact angle was calculated by using Young/Laplace equilibriums with computer software. The Water Contact Angle (WCA) test was finished by evaluating the average of the angle values saved throughout 9 seconds with the camera. This process was performed 10 times for each nonwoven fiber.

The mechanical properties of all the nonwoven nanofibers were tested with Lloyd Instruments LRX Plus branded pulling device running at 1:10 mm/min pulling velocity and 5kN load due to the ASTM D882 standard. For the tensile test, 5 samples of 50 mm x 15 mm from each electrospun nonwoven were used and the results were averaged.

Antibacterial activity test

The in vitro antibacterial effect against Gram-positive bacteria (*S. aureus* ATCC 29213), and Gram-negative bacteria (*E. coli* ATCC 25922 and *P. aeruginosa* ATCC 27853) of PLA/TPU-Ag electrospun webs was analyzed

Table 2: ηr and Flow Time (sec) values of solutions

Solutions	Flow time (sec)	η_r
CF	7.1	-
DMF	10.1	-
CF/DMF (8/2 v/v)	8.3	-
Neat PLA	11.6	1.4
Neat TPU	27.3	3.3
2AgTPU	31.7	3.8
5AgTPU	35.5	4.3
10AgTPU	41.1	5.0

according to agar plate colony counting procedure that is a quantitative technique [18, 19]. The antibacterial test has been carried out appropriately to the AATCC-100 standard [20]. Initially, the sterilized process applied both sides of nanomaterials sized 1 cm x 1 cm for 30 minutes under UV light. The nanofiber samples were cut from three different regions of each nanomaterial for each bacterial strain. In other words, three samples of each nanomaterial were prepared for each bacterial species. Later, Mueller Hinton Agar (MHA) and Mueller Hinton Broth (MHB) (Merck, Germany) prepared for 15 min in the autoclave at 121°C. Bacteria were grown at 37°C overnight on MHA. Bacteria increased on MHA were suspended in 3 ml MHB. Next, sterilized electrospun webs accommodated individually in the 24-well plate were inoculated with 600 µL of formed bacterial suspension (10^4 CFU/mL^{-1}). After, they were inoculated in 20 µL MHA from each well at 0h, 6h, 12h, and 24h incubated overnight at 37°C. Bacteria bred on agar plates were counted. The applied processes to determine the antibacterial activity at 0h, 6h, 12h, and 24h time intervals against each bacterial species of each nanomaterial were repeated three times. The mean and standard deviation of the results were calculated. The antibacterial activity (%) of electrospun webs is calculated according to the following "Equation (2)":

$$Antibacterial\ Activity\ (\%) \frac{A-B}{A} \text{ x } 100 \qquad (2)$$

Where *A* is the average bacteria count of the untreated bicomponent nanofibers control material; *B* is the mean count of bacteria per hour with the least count of bacteria except the 0 hours.

Cytotoxicity test

The cytotoxicity properties of the PLA/TPU-Ag webs have been analyzed on mouse fibroblast cell line (L929) by WST-1 assay [12] with direct contact operation. Initially, each side of the nanomaterials has been sterilized for 30 min under UV light. L929 cells were cultured in high glucose DMEM attached with 1.4 % L-glutamine, 100 µg/mL of streptomycin, 100 U/mL penicillin, and 10% fetal bovine serum. On electrospun webs in the 24-well plate have been placed L929 cells. The processed plate was cultured at 5 % CO_2 and 37ºC. Later, after 24 hours of incubation, 50 µL of WST-1 solution (BioVision Incorporated, USA) has been added to each well. The plate was continuously incubated for 2 h at 37ºC, after shaking fully for 1 min, measured of OD value at wavelength 450 nm with a microplate reader (Multiskan FC, Thermo Scientific).

The well plate did not contain the bicomponent webs as a negative control, cells with 1 % (v/v) Triton X-100 (Sigma) and 500 µg/ml Geneticin (Gibco) as a positive control, and an equal volume of culture medium that contained WST-1/ECS solution in an empty well as a blank well have been prepared.

This cytotoxicity test was repeated 3 times. Cell viability (%) has been calculated following "Equation (3)":

$$Cell\ viability\ (\%) = \frac{A_b\ sample - A_b\ blank}{A_b\ control - A_b\ blank} \text{ x } 100 \qquad (3)$$

Where *Ab* sample is the nanofiber absorbance, *Ab* control is the absorbance of the negative control, and *Ab* blank is the absorbance of the blank.

RESULT AND DISCUSSION

Surface micrographs

SEM images of all electrospun mats at 2000x magnification are shown in Fig. 1. It is seen those pure nanofibers and bicomponent nanofibers are bead-free, homogeneous, and with a smooth surface. Evaluating Fig. 2, which contains the average fiber diameters of the fibers, the PLA in the core, and the TPU in the shell (coPLAshTPU) bicomponent fiber thickness is almost the same as that of the neat TPU fiber. This situation shows that the structure of the TPU fiber in the outer shell surrounding the bicomponent fiber is dominant over the thickness of the bicomponent fiber diameter. Error bars provide information about the average fiber thicknesses. Except for neat PLA (±75nm), the average diameter of other fibers increases and decreases in the range of ±150 nm. After AgNPs were added, there was an increase in all the fibers compared to the coPLAshTPU nanofiber. This is due to the viscosity increase in the TPU-Ag NPs polymer

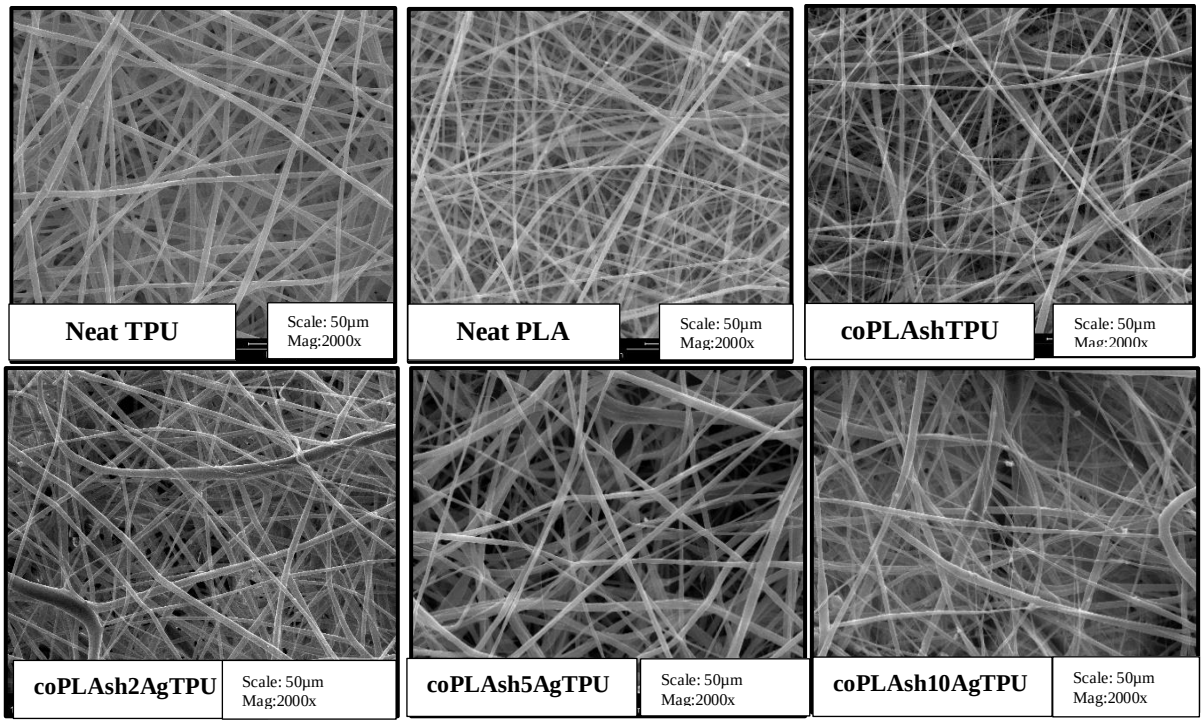

Fig 1: SEM micrographs of all the electrospun fibers (Scale: 50µm, Mag:2000x)

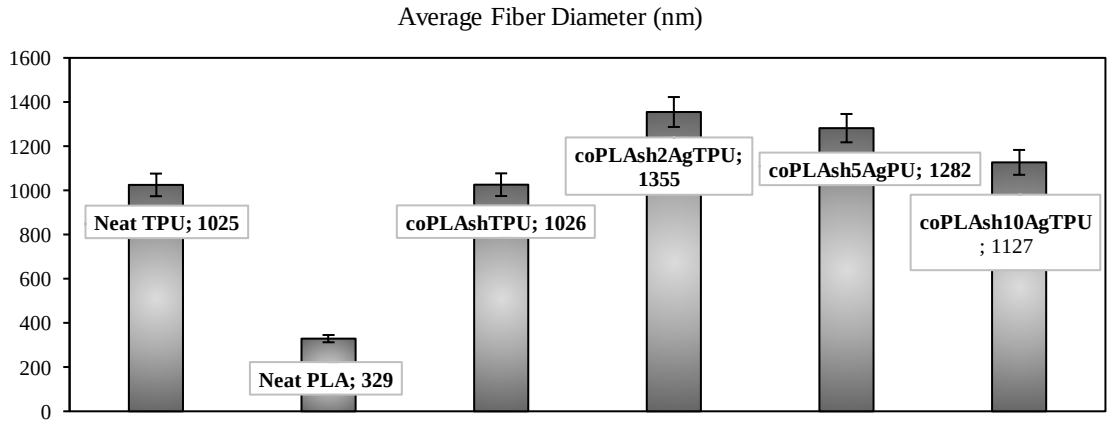

Fig 2: Diameter measurement of all the electrospun fibers

solution prepared. The relative viscosity measurements of the solutions affecting the bicomponent fiber diameters are shown in Table 2. Viscosity increased with the increasing amount of Ag NP. Due to the high viscosity of the TPU-Ag NPs solutions in the outer shell, the fiber diameters have thickened. High viscosity means more interaction between solvent and polymer molecules, and thus, when the solution is stretched with the effect of charges, the solvent molecules will tend to diffuse into complex polymer molecules, and thus the tendency of solvent molecules to aggregate under the influence of surface tension will decrease [21].

On the other hand, because of the hydrophobic structure of TPU and the evident density difference between Ag and polymer, the distribution of AgNPs in the TPU matrix may have been difficult [22]. The density of Ag is very high (10.53 g/cm^3) compared to polymers with a density of around 1.0 g/cm^3 and therefore silvers are inclined to settle during the production of polymer composites [23, 24]. However, as the amount of Ag NPs in the TPU-Ag NPs solutions increased, results like the literature were obtained, with a steady decrease in

Table 3. Presence of Ag NPs obtained from EDX analysis

Samples	coPLAsh2AgTPU	oPLAsh5AgTPU	coPLAsh10AgTPU
Ag NPs amount (wt %)	1.97	.08	8.83

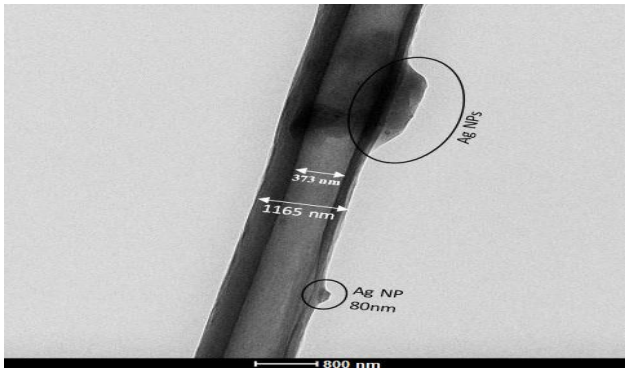

Fig 3. TEM image of the coPLAsh10AgTPU nanofiber

the average diameters of bicomponent nanofibers [25]. However, the mean diameter of the coPLAsh10AgTPU bicomponent nanofiber with the highest Ag NPs ratio was not as thin as that of the control sample coPLAshTPU nanofiber. The reason for this is that the conductivity of the solutions is linear with the conductivity of the nanofiber surfaces, the higher the Ag NPs ratio, the higher the conductivity of the solutions. With the increasing amount of Ag NP, the conductivity of the solutions increases, and the resulting nanofibers become thinner.

To prevent the effect of changing electrospinning method conditions on fiber properties, electrospinning process conditions were kept constant in this study. However, the optimum conditions provided by the solution viscosity and solution conductivity varying with the increase in the amount of Ag NPs made the average fiber diameters thinner. Because, in solutions with high conductivity, the charge-carrying capacity increases due to the excess of ions, and in this case, more voltage occurs with the applied electric field. Thus, the jet lengthens and with the elongating jet, finer fibers are formed in the collector.

The TEM image showing the core and shell parts of the coPLAsh10AgTPU nanofiber were given in Fig. 3. The PLA fiber inside the bicomponent structure has shown a similar diameter value to the measurement of the neat PLA fiber. These results showed that the diameter properties of bicomponent nanofibers were compatible with neat PLA and neat TPU nanofibers. In addition, while Ag NPs structures were about 35 nm, it was seen in the TEM image that Ag NPs found only in the shell settled as Ag NPs with higher diameters because of agglomeration. In addition, Ag NPs distributions on bicomponent electrospun fibers are shown in Fig. 4 with dark images obtained from SEM micrographs. With the proportional increase of Ag NPs in the structure, their distribution on the surface increased. Although Ag NPs are distributed homogeneously on the surface in general, agglomerations have been seen in some regions on SEM micrographs too like the TEM Fig.. The presence of these agglomerations was associated with the fact that the Ag NPs ratios (%) obtained in the EDX analysis taken from a specific area of the fiber in Table 3 were almost the same as the ratio added into the solution but gave slightly different results.

FTIR analysis

FTIR-ATR spectra containing all the electrospun web's chemical bond structures are shown in Fig. 5. The 1708 cm^{-1} (neat TPU), the 1654 cm^{-1} (neat TPU), and the 1674 cm^{-1} (neat PLA) peaks formed a single peak in the structure of bicomponent fibers at 1701 cm^{-1}. The peak around 1700 cm^{-1} that was observed to C=O was shown the stretching of urethane. Peaks corresponding to the absorption of NH, C=O, and C−O were respectively seen at about 3314 cm^{-1}, 1701 cm^{-1}, and 1221 cm^{-1} which demonstrated the bicomponent nanomaterials containing the urethane (NHCOO) group [26]. The other characteristic peaks of Neat TPU are the 2936 cm^{-1} peak that shows the CH_2 tensile vibration, the 2855 cm^{-1} peak at CH_2, the 1600 cm-1 peak that follows aromatic C=O group oscillations, 1530 cm-1 at N-H, 1413 cm^{-1} at (C=O-O) and 1311 cm^{-1} peak that indicated the (N-H) + (C-N) + (C-H) vibrations [27].

The characteristic peak of PLA is C = O stress vibration at 1750 cm^{-1} peak. In addition, other peaks of pure PLA fiber belong to the O-H at 2998 cm^{-1}, the CH_3 at 1368 cm^{-1}, the carbonyl group (C-O-C) at 1269 cm^{-1} peak, the (O-C=O) at 1187 cm^{-1} peak, the 1125 cm^{-1} peak at (C-O-C) group and the (C-O-H) vibrations at 1084 cm^{-1} peak. All peaks sighted at neat TPU and neat PLA were observed on all bicomponent nanofibers too. The 1368 cm^{-1} peak seen

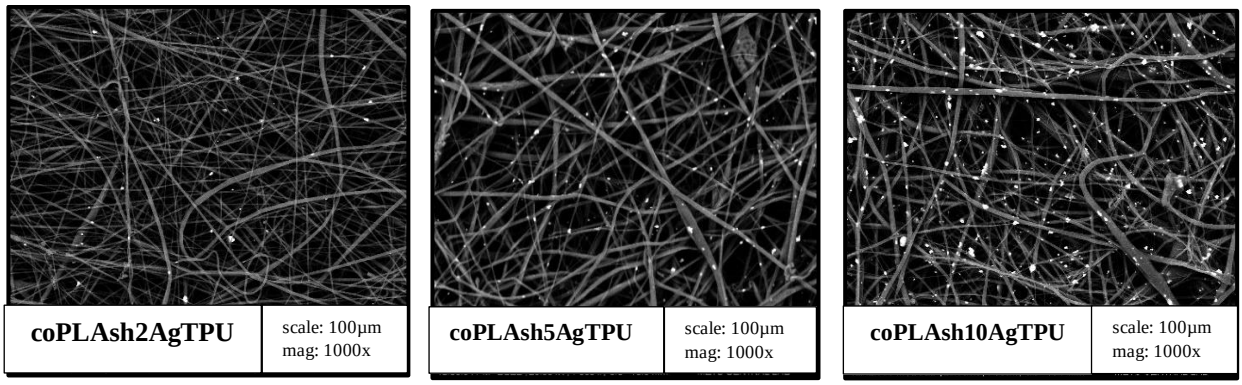

Fig 4. Ag NPs distribution in the shell (scale: 100µm, mag: 1000x)

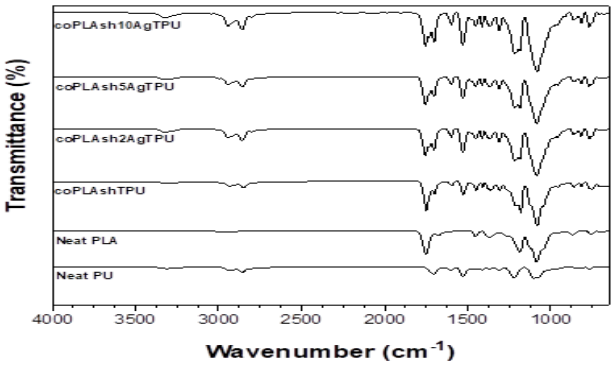

Fig 5. FTIR spectra of all the electrospun fibers

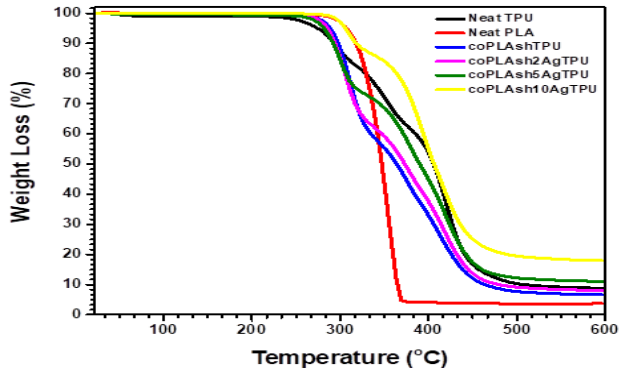

Fig 6: TGA curves of all the electrospun fibers

in both PLA and TPU belong to the CH_3 group. This peak has been lost in all bicomponent nanofibers. At these nanofibers were observed two new peaks as 1379 cm^{-1} and 1357 cm^{-1}.

Also, the 1098 cm^{-1} peak seen at neat TPU and 1084 cm^{-1} peaks sighted at neat PLA were observed at 1084 cm^{-1} as a single peak by sliding in bicomponent nanofibers. In addition, 1036 cm^{-1} peaks seen in neat PLA and 1070 peaks seen in neat TPU were seen at 1036 cm^{-1} as a single peak by sliding in bicomponent nanofibers. The peaks are seen between 900-750 cm^{-1} and also belong to C-H vibrations. These peaks have been seen at all nanofibers.

In this study, during the coaxial bicomponent electrospun mats manufacture process, the polymer solutions gushing of the syringe tip simultaneously create an only jet together. This jet forms an interaction between the polymer solutions on account of the influence of t he electrical area. This operation has caused peak shifts, new peak formations, and peak loss, and has changed the vibration behavior of the bonds. The electrical area taking place pending the electrospinning operation has triggered the interplay among the polymer solutions. If a chemical response emerged when an external voltage is applied, it can be foretold that an electrochemical reaction occurs between the polymer solutions that create a only jet. For, in an electrochemical reaction, the electrical charge of an atom or ion alters as a consequence of electron transfer. PLA and TPU are partially harmonious polymers [28] and are inclined to interact readily with each other. Therefore, owing to the interaction between the polymers with the voltage application from the external pending the coaxial electrospinning process, it has been indicated that the electrochemical reaction occurred for a short time at the jet tip.

TGA analysis

TGA curves of all nanofibers have been shown in Fig. 6. The thermal properties of the coPLAshTPU nanofiber were observed as a single structure that combines the properties of both nanofibers. The temperature curves of all bicomponent nanofibers have been realized in three steps compared to neat TPU. This matter is due to the presence of hard and soft segments in the structure of the TPU polymer. So, hard and soft parts decompose at different temperatures [8].

Table 4: The thermal decomposition values of all the electrospun fibers

Sample Codes	Tmax (°C)			T_{deg5} (°C)	Residue 600°C (%wt)
	1st step	2nd step	3rd step		
Neat TPU	297.19	352.13	420.08	274.54	8.82
Neat PLA	354.65	-	-	307.01	3.71
coPLAshTPU	311.17	375.62	412.95	288.80	6.68
coPLAsh2AgTPU	305.28	376.93	416.81	285.63	8.11
coPLAsh5AgTPU	300.11	380.63	419.64	281.67	11.07
coPLAsh10AgTPU	309.77	392.82	419.04	306.00	18.00

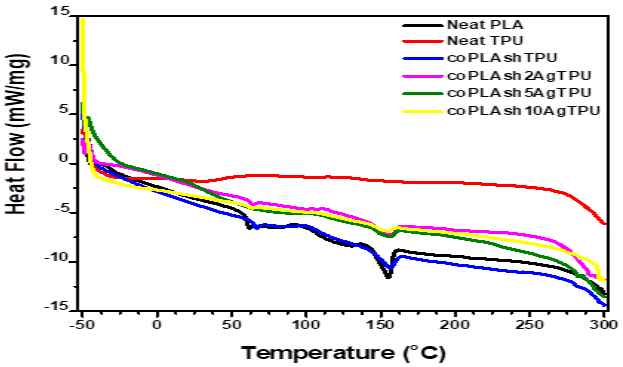

Fig 7: DSC curves of all the electrospun fibers

The increase in the first and second steps of coPLAshTPU according to neat TPU has been due to the structure of neat PLA, which has high heat resistance. However, the decomposition values of electrospun mats have been shown in Table 4. The T_{deg5} value of the electrospun mats shown in Table 4, describes as decomposition temperature corresponding to the mass loss of 5% by weight on the TGA curves. Moreover, the derivative (DTG) curve of the electrospun mats has been examined as well as the TGA curves. So, also the Tmax temperature values corresponding to the maximum degradation rate acquired from the DTG derivative curves are shown in Table 4. When Table 4 is examined, the temperature of the 2nd degradation step increased steadily with the increase in the amount of Ag NPs in bicomponent nanofibers. It has been considered that owing to the entangled agglomeration of the remaining Ag NPs among the nanofibers, the decompose temperature (T_{max2}) of the nanofibers in the 2nd step has increased.

Ag NPs agglomerated between the fibers due to the rapid but slow release of the Ag NPs in the outer part of the bicomponent increasing the thermal strength of the nanofiber structure. When Ag NPs start to be released, the agglomerated structure will be released late and its temperature resistance will increase. T_{max3} temperatures of bicomponent nanofibers showed similar temperature values with neat TPU. This situation is associated with the neat TPU characteristic decomposition curve and T_{max3} temperature. Due to the hard segment bond structures in neat TPU nanofibers, T_{max3} temperatures in the structure did not change.

In addition, when the T_{deg5} temperature was evaluated, mass loss was experienced in all bicomponent electrospun mats at 285°C (±4) temperature which is a value between neat PLA and neat TPU. The coPLAsh10AgTPU nanofiber has shown the closest and highest T_{deg5} value to that of neat PLA with a temperature of 306°C. It was concluded that the coPLAsh10AgTPU nanofiber containing the highest amount of Ag NPs showed the highest T_{deg5} value thanks to the high-temperature resistance of the Ag NP structure. Thus, when the residual amounts of bicomponent nanofibers were compared with the residue amount of coPLAshTPU nanofibers, Ag NP percentage was added to the structure in Ag NP doped nanofibers also preserved their presence at 600°C. The coPLAshTPU nanofiber left a residue of 6.68% between the residue amount of neat PLA and neat TPU. The amount of residues increased linearly with the increase of Ag NP. It has been approved that the Ag NP structure remains as it was at the end of 600°C and that the PLA and TPU structures have degradation and loss of mass. The TGA results have confirmed that the excess amount of Ag NP residue of approximately 1% in the coPLAsh10AgTPU nanofiber according to that of the coPLAshTPU may be due to the accumulation in the tested area as a result of agglomerations that were seen on the TEM Fig..

DSC analysis

DSC curves showing the thermal properties of nanofibers are given in Fig. 7. It has been determined

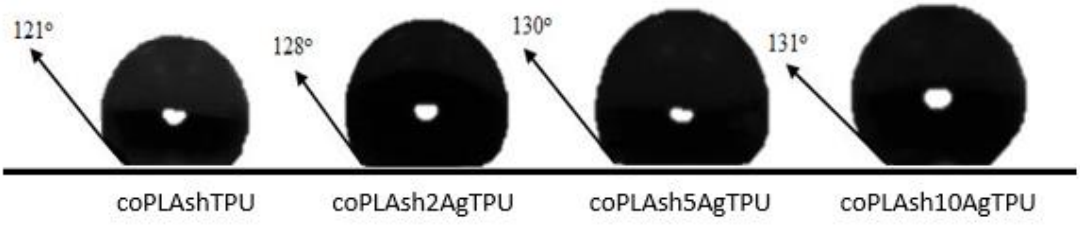

Fig 8: Contact angle (°) values of all the electrospun fibers

which T_g value of neat PLA nanofibers was 59°C and the Tm temperature was 154°C. In addition, It has been found that the T_g temperature of neat TPU nanofiber was (-40°C) and two different T_m values were 30°C for the soft segment and 110°C for the hard segment of neat PU nanofiber [27]. All of the bicomponent nanofibers obtained have shown similar curves to the DSC curve of neat PLA. Thus, it has been indicated that the structure in the core dominates the DSC thermal properties. No striking differences have been observed in the DSC temperature values of nanofibers. This is an expected effect. In the production of bicomponent nanofibers, no continually ongoing chemical event could cause changes in the characteristic T_g and T_m values of the polymers. For this reason, the thermal properties of both neat PLA and neat TPU nanofibers in bicomponent structures showed efficiency as individuals in a single structure at the same time. The active presence of neat PLA and neat TPU nanofibers has been proven in all bicomponent fibers with DSC results.

Contact angle analysis

The contact angle values that give information about the water-repellent properties of all nanofibers are shown in Fig. 8. On a smooth solid surface, the contact angle can be as high as ~120°. This is possible on material surfaces with very low free surface energy (eg Teflon). To obtain a contact angle greater than this value, the surface must have a rough structure to a certain extent (micro/nano). In this way, the free surface energy of the surface can be reduced more [29]. In our previous study, neat TPU and neat PLA showed contact angle values of 120 and 121, respectively [8]. The coPLAshTPU nanofiber showed hydrophobic properties at approximately an angle of 120°. These fibers are nanomaterials whose surfaces are smooth and do not contain any material that will create any nano/micro-size roughness in their structure. However, the surface contact angle increased with the increase in the amount of Ag NP added to the structure. Ag NP doped bicomponent nanofibers showed quite high hydrophobic properties with an angle of 130° (±2). When the coPLAshTPU nanofiber is compared with Ag NP added bicomponent nanofibers, as the amount of Ag NP in the structure increases, there is an increment of 4.13%, 7.44 %, and 8.26% respectively. In the structure of these bicomponent materials, there are Ag NPs of approximately 35 nm in size or agglomerated. The presence in the outer shell of the bicomponent nanofiber structure of Ag NPs has created an invisible nano-sized roughness. The protrusions seen in this outer shell are confirmed by dark images obtained from SEM analysis and TEM images.

The leading point in wound healing is keeping the wound area is moist. Thanks to the high porosity of the natural structure of nanofibers, a high ratio of humid vapor is transferred to the wound surface. In dry wounds, the TPU structure declines the vapor loss and encumbers the wound surface from drying out, so TPU supplies the wound humidity [30]. The low wettability properties of PLA with a hydrophobic structure are more pronounced in the electrospun morphology of PLA nanofiber [31]. In this study, the PLA/TPU-AgNP bicomponent electrospun mats are suggested for the treatment of dry wounds. Moreover, according to the antibacterial test results, it is thought that the dressing will be changed at the end of 24 hours, which can also enable its use in wounds with quite poor exudate.

It is expected that the coPLAsh5AgTPU and the coPLAsh10AgTPU nanofibers will ensure greater patient comfort when used as wound dressings, courtesy of their high water-repellency property. For example, when the surface of the limb that is in frequent contact with water, such as the hand, is clothed, the open wound surface, which will comfort daily life, will be hindered from contact with water.

Mechanical analysis

Comparing the tensile stress at max load (MPa) and

Table 5: The values obtained from mechanical test results

Samples	Tensile Stress at Max Load (MPa)	Tensile Strain at Max Load(%)
Neat TPU	6.73	272.8
Neat PLA	0.33	24.7
coPLAshTPU	1. 37	46.26
coPLAsh2AgTPU	1.98	47.32
coPLAsh5AgTPU	2.36	56.70
coPLAsh10AgTPU	2.53	66.84

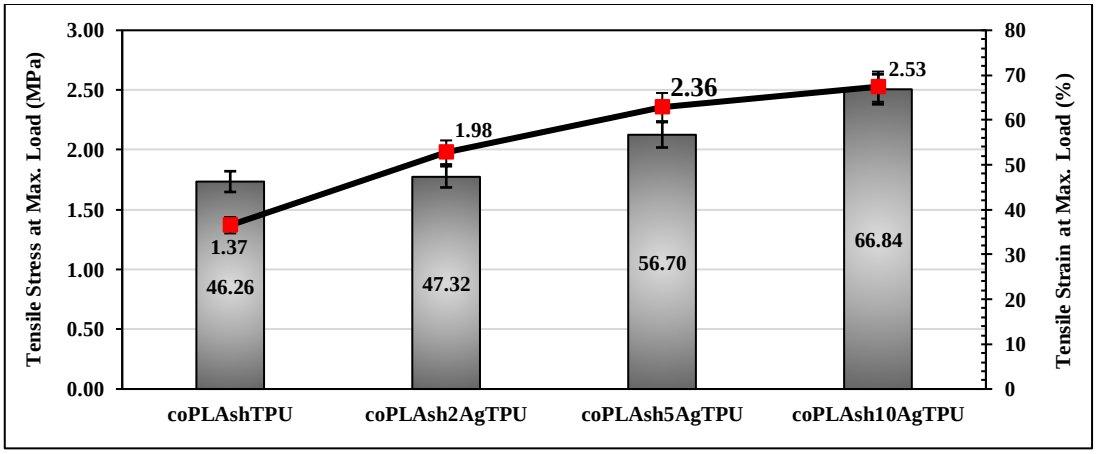

Fig 9: Mechanical properties of all the electrospun fibers

the tensile strain at max load (%) of all electrospun mats have been examined in Fig. 9. Also, the values obtained from mechanical test results have shown in Table 5. While the hard parts of the neat TPU electrospun mat enhance the tensile stress, the loose parts of the neat TPU electrospun mat boost the extension in the structure. The neat PLA nanofiber shows physical properties like being brittle and weak. The PLA has low strength and elongation behavior [32]. The coPLAshTPU nanofiber showed strength with a value of 1.37 MPa and elongation with a value of 46.26% behavior between the mechanical values of neat TPU and neat PLA nanofibers. All the nanostructured bicomponent nanofibers have improved mechanical properties. As the amount of Ag NPs added to the structure increased the strength and elongation behavior of bicomponent electrospun webs increased linearly [30, 33]. The fiber with the highest tensile strength and elasticity was coPLAsh10AgTPU nanofiber with values of 2.53 MPa and 66.84%, respectively. The neat TPU nanofiber had high elasticity and strength values. In addition, patient comfort will be provided when the obtained nanofibers are used as a wound dressing. Thus, it is thought that it will be comfortable to move the covered body parts. Moreover, the movement of the patient will not be restricted and the wound will heal.

Antibacterial activity

It has been viewed that the Ag NPs were extremely effective against studied bacterium species by antibacterial activity (%) results. Thus, antibacterial effective wound dressing has been successfully obtained against *S. aureus*, *P. aeruginosa*, and *E. coli*. The *E. coli* view on agar for electrospun mats has been given in Fig. 10. In addition, counts of E. coli and antibacterial activity (%) of electrospun mats have been dedicated in Table 6. For 0h, 6h, 12h, and 24h, the numerous *E. coli* reproductive for the coPLAshTPU nanofiber has been expected. Whereat this nanofiber without Ag NPs has been determined as a control electrospun mat. The Ag NPs demonstrated antibacterial features by reacting with plasma structures and the cell barriers of bacteria [34, 35]. When 2% Ag NPs were used, *E.coli* bacteria were fully demolished at the end of the 12th hour. However, as the amount of Ag NPs in the bicomponent nanofiber structure increased, and the 100% antibacterial effect was acquired in a shorter time. The 5% and 10% Ag NPs added electrospun mats, *E.coli*

Table 6: The bacterium count of E. coli and antibacterial activity (%) for mats

Samples	0 hour	6 hour	12 hour	24 hour	Antibacterial Activity (%)
coPLAshTPU	Average: 74 Std dev: 1.73	Average ~10^3(countless)	Average ~10^4(countless)	Average ~10^5(countless)	-
coPLAsh2AgTPU	Average 301 Std dev: 6.11	Average 99 Std dev: 3.60	Average 0 Std dev: 0.00	Average 102 Std dev: 2.08	For 6h 100
coPLAsh5AgTPU	Average 200 Std dev: 4.0	Average 0 Std dev: 0.00	Average 0 Std dev: 0.00	Average 84 Std dev: 4.58	For 6h and 12h 100
coPLAsh10AgTPU	Average 61 Std dev: 3.05	Average 0 Std dev: 0.00	Average 0 Std dev: 0.00	Average 32 Std dev: 5.29	For 6h and 12h 100

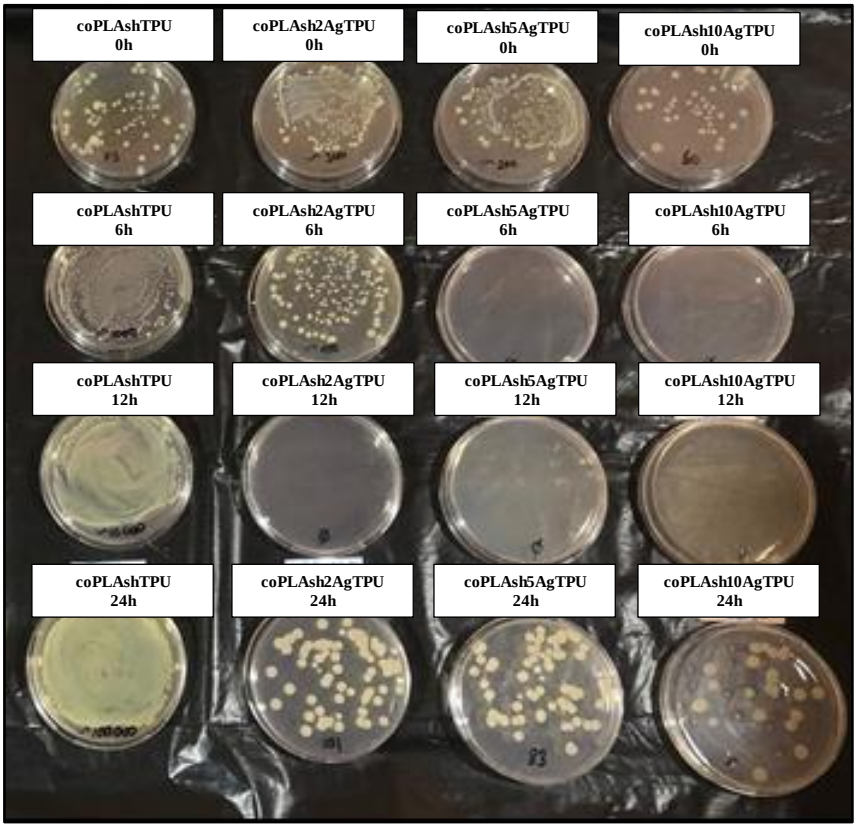

Fig 10: The E. coli view on agar for electrospun mats (respectively from left to right: coPLAshTPU, coPLAsh2AgTPU, coPLAsh5AgTPU, coPLAsh10AgTPU) (respectively from top to bottom : 0h, 6h, 12h, and 24h)

The *P. aeruginosa* view on agar for nanofibers has been shown in Fig. 11. In addition, the bacterium count of *P. aeruginosa* and the antibacterial activity (%) of nanofibers has been given in Table 7. During 0h, 6h, 12h, and 24h, countless *P. aeruginosa* breeding for the coPLAshTPU electrospun mat has been expected. These nanofibers without AgNPs have been used as control electrospun mats for *P. aeruginosa*. When 2% and 5% Ag NPs have been used *P.aeruginosa* bacteria have fully vanished at the end of the 12th hour [36]. This antibacterial activity has been maintained until the end of the 24th hour. For the electrospun mat with 10% Ag NPs added,

Table 7: The bacterium count of P. aeruginosa and antibacterial activity (%) for mats

Samples	0 hour	6 hour	12 hour	24 hour	Antibacterial Activity (%)
coPLAshTPU	Average 41 Std dev: 1.00	Average ~$2x10^3$ countless	Average ~10^4 (countless)	Average ~10^5 (countless)	-
coPLAsh2AgTPU	Average 302 Std dev: 11.59	Average 4 Std dev: 0.57	Average 0 Std dev: 0.00	Average 0 Std dev: 0.00	For 12h, and 24h 100
coPLAsh5AgTPU	Average 157 Std dev: 7.02	Average 2 Std dev: 0.00	Average 0 Std dev: 0.00	Average 0 Std dev: 0.00	For 12h, and 24h 100
coPLAsh10AgTPU	Average 106 Std dev: 7.76	Average 0 Std dev: 0.00	Average 0 Std dev: 0.00	Average 0 Std dev: 0.00	For 6h, 12h, and 24h 100

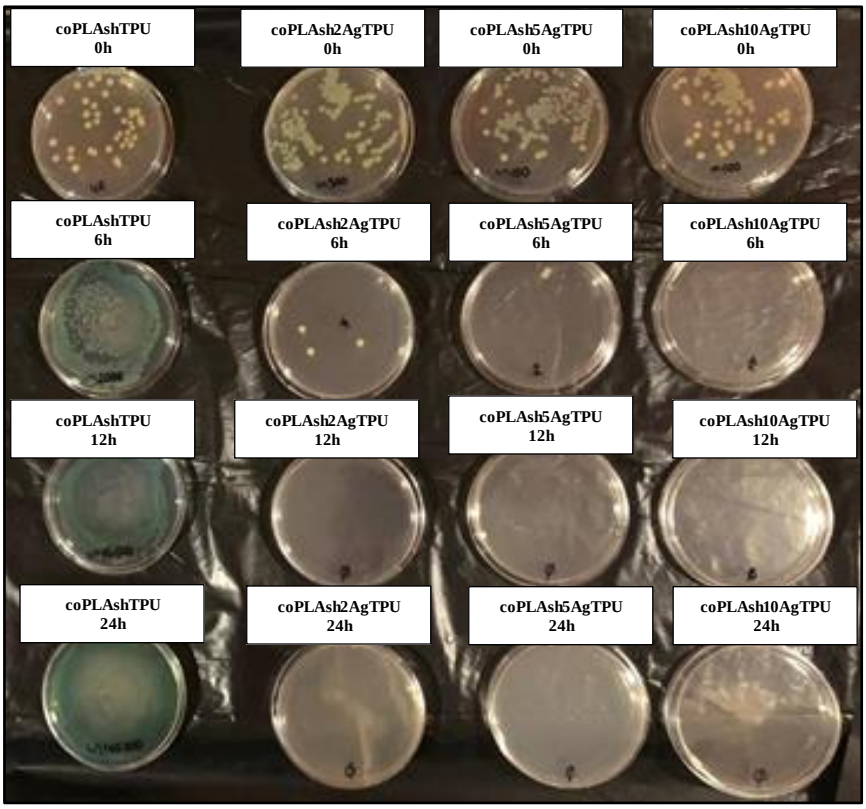

Fig 11: The P. aeruginosa view on agar for electrospun mats (respectively from left to right: coPLAshTPU, coPLAsh2AgTPU, coPLAsh5AgTPU, coPLAsh10AgTPU) (respectively from top to bottom : 0h, 6h, 12h, and 24h)

P. aeruginosa was annihilated at the end of the 6th hour. The 100% antibacterial activity was acquired in a shorter time as the amount of Ag NPs in the nanofiber structure increased. The coPLAsh10AgTPU electrospun mat, like other bicomponent nanofibers, continued its 100% antibacterial activity for 24 hours. It has been recommended appropriate to renew them at the end of every 24 hours when these nanofibers are used as an antibacterial effective wound dressing for *P. aeruginosa*. The S. *aureus* view on agar for nanofibers has been viewed

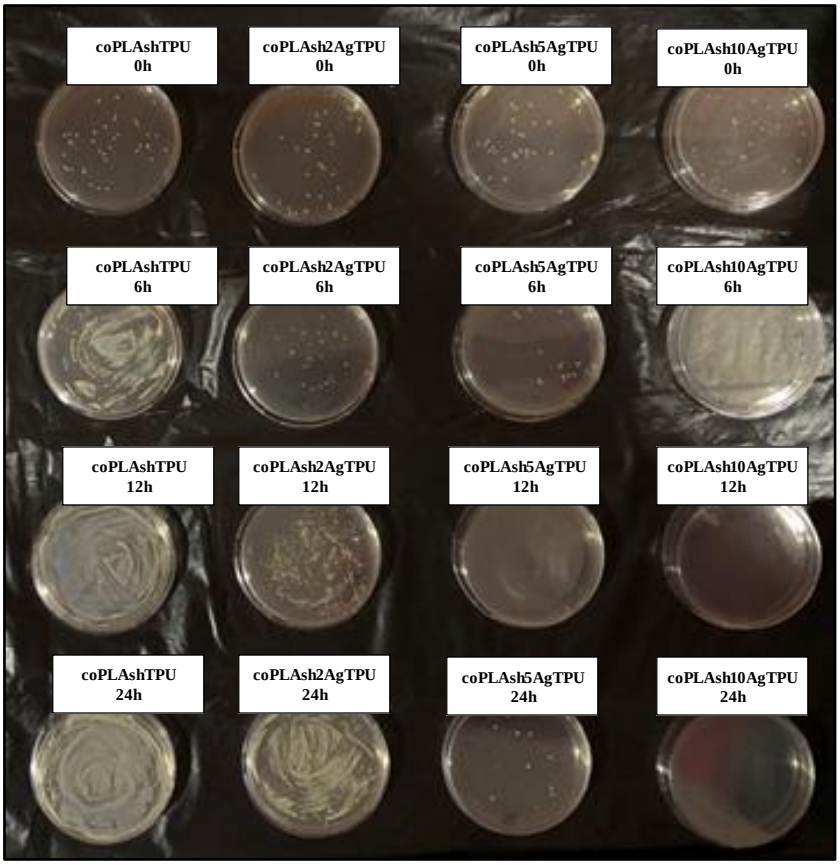

Fig 12: The S. aureus view on agar for electrospun mats (respectively from left to right: coPLAshTPU, coPLAsh2AgTPU, coPLAsh5AgTPU, coPLAsh10AgTPU) (respectively from top to bottom : 0h, 6h, 12h, and 24h)

in Fig. 12. In addition, the bacterium count of S. *aureus* and antibacterial activity (%) for nanofibers has been shown in Table 8. During 0h, 6h, 12h, and 24h, countless *S. aureus* reproduction for the coPLAshTPU electrospun mats was anticipated. This nanofiber without Ag NPs was used as a control nanofiber sample for *S. aureus*. However, bacterium breeding could not be blocked for the coPLAsh2AgTPU electrospun mat in 24 hours even. The percent of silver in the structure of this nanofiber has been not sufficient to decrease or entirely overthrow *S. aureus*. A regular increment for *S. aureus* for it has been seen from the 0th hour. Unlike the results of other bacterium types, a notable increment in the count and breeding speed of *S. aureus* has been observed. The cell wall of Gram-positive *S. aureus* is thick by its nature. This behavior protects the bacteria from external influences and thus, Ag NPs cannot be easily diffused into the inner structure of the bacterium [37]. For *S. aureus*, 5% and 10% Ag NPs added mats indicated 100% antibacterial activity at the end of the 12th hour. While bacterium breeding has been observed in the coPLAsh5AgTPU electrospun mat at the end of the 24th hour, the coPLAsh10AgTPU mat maintained its 100% antibacterial effect up to the end of the 24th hour. For *S. aureus* when these nanofibers are used as a wound dressing, the coPLAsh5AgTPU electrospun mat should be renewed at the end of the 12th hour and the coPLAsh10AgTPU electrospun mat should be renewed at the end of the 24th hour.

The coPLAsh5AgTPU and the coPLAsh10AgTPU nanomaterials, which display 100% antibacterial activity as the bicomponent single structure for three bacterium types, are suitable for wound dressings.

Cytotoxicity

Antibacterial test results have shown the usability of bicomponent electrospun mats as an antibacterial effective wound dressing. If it is a cytotoxicity test, it definitively states nanofibers this usability as tissue scaffolds or a wound dressing. The most significant test that describes the usability of a material as a wound dressing or tissue

Table 8: The bacterium count of S. aureus and antibacterial activity (%) for mats

Samples	0 hour	6 hour	12 hour	24 hour	Antibacterial Activity (%)
coPLAshTPU	Average: 39 Std dev: 1.00	Average ~10^4 (countless)	Average ~10^5 (countless)	Average ~10^5 (countless)	-
coPLAsh2AgTPU	Average: 33 Std dev: 1.15	Average: 31 Std dev: 0.57	Average: 503 Std dev: 15.27	Average ~10^4 (countless)	-
coPLAsh5AgTPU	Average: 34 Std dev: 2.00	Average: 23 Std dev: 1.52	Average 0 Std dev: 0.00	Average: 15 Std dev: 1.00	For 12h 100
coPLAsh10AgTPU	Average: 25 Std dev: 1.73	Average: 18 Std dev: 0.57	Average 0 Std dev: 0.00	Average 0 Std dev: 0.00	For 12h and 24h 100

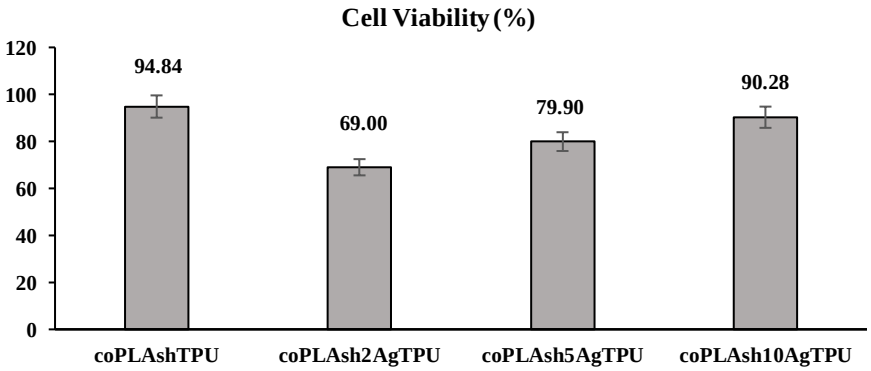

Fig 13: The cell viability (%) graphs of mats

scaffold is the cytotoxicity test. Also, the reason for stopping at the end of the 24 hours of the cytotoxicity test is that the antibacterial activity is exhausted at the end of the 12th and 24th hours.

The cell viabilities (%) percent of electrospun mats are shown in Fig. 13. The coPLAshTPU bicomponent electrospun mat has been evaluated as the negative control sample. Since TPU and PLA polymers are biocompatible, the highly toxic effect was not anticipated. In addition, the coPLAshTPU mat has indicated cell viability with a 94.84% value.

The toxic effects of the positive control were calculated as a 55.15% value. The obtained nanofibers were approved as non-toxic structures, providing that the cell viability (%) was this value and above. If not, the cell viability is above 70%, it is indicated that the produced materials cannot be used for medical areas such as tissue scaffolds or wound dressing [12]. So, the coPLAsh2AgTPU bicomponent mat is at a limit value of 69% for wound dressing use. If accepted to be a tolerable value, it may be used as an antibacterial wound dressing for *E. coli* and *P. aeruginosa*. But it would be much more suitable to use as a wound dressing 5% and 10% Ag NP-doped mats that had respectively 79,90% and 90,28% of cell viability.

As a result, dressing and scaffold nanomaterials that may be used as nanofiber structures for three bacterium types are coPLAsh5AgTPU and coPLAsh10AgTPU mats. While providing 100% antibacterial activity, they also promote cell viability. *Movahedi et al* have reported that the thinned mats are effective in cell growth [38]. It has been determined that coPLAsh5AgTPU is the most useful mat for wound dressing when it is evaluated as a structure that conduces to high cell viability and 100% antibacterial activity for three bacterium types with low Ag NP ratio. However, this nanofiber also has high elasticity and strength, which may satisfy in terms of mechanical

properties. In that case, coPLAsh5AgTPU nanomaterial is suitable to use as a wound dressing by renewing it every 12 hours as it is 100% antibacterial for *E.coli*, *P. aeruginosa*, and *S. aureus* and harmless to health.

CONCLUSIONS

In this report, core PLA and shell TPU-Ag bicomponent nanofibers have been successfully obtained to obtain an antibacterial effective wound dressing. PLA and TPU polymers without mixing were used together as a single structure while preserving their individual properties. These novel nanomaterials have been designed to be used to cover dry wounds owing to their high hydrophobic character containing high antibacterial activity and high cell viability. It has been indicated that the 2% Ag NP-doped bicomponent nanofiber with cell viability at the limit value of 69% (if accepted to be a tolerable value) can be used as a wound dressing, provided that it is renewed every 12 hours for *E.coli* and every 24 h for *P. aeruginosa*. However, it would be more appropriate and safer to use as a wound dressing the 5% and 10% Ag NP doped bicomponent nanofibers that have high antibacterial effects for all three bacterial species and with cell viability rates of approximately 80% and 90% respectively if wound dressings are renewed every 24 hours. It has been emphasized that high patient comfort will be provided through the high hydrophobic character and high mechanical behavior of the bicomponent electrospun mats produced. It has been reported that freedom of movement will not be restricted or that it can be used safely and easily on body surfaces that are in frequent contact with water. In addition, it is predicted that bicomponent nanofibers will accelerate wound healing through their superior properties.

Received :Dec. 05, 2022 ; Accepted : Feb. 20, 2023

REFERENCES

[1] Aziz T., Farid A., Haq F., Kiran M., Ullah A., Zhang K., Li C., Ghazanfar S., Sun H., Ullah R., Ali A., Muzammal M., Shah M., Akhtar N., Selim S., Hagagy N., Samy M., Al Jaouni S.K., A Review on the Modification of Cellulose and Its Applications, *Polymers*, **14(15)**: 3206-3215 (2022).

[2] Alharbi H., Luqman M., Khalil K., Elnakady Y.A., Abd-Elkader O., Rady A., Alharthi N., Karim M., Fabrication of Core-Shell Structured Nanofibers of Poly (Lactic Acid) and Poly (Vinyl Alcohol) by Coaxial Electrospinning for Tissue Engineering, *European Polym. J.*, **98**: 483-491 (2018).

[3] Alghoraibi I., Alomari S., "Different Methods for Nanofiber Design and Fabrication", Springer, (2018).

[4] Wang Q., Zhu L., Polymer Nanocomposites for Electrical Energy Storage, *J. Polym. Sci. Part B: Polym. Phys.*, **49(20)**: 1421-1429 (2011).

[5] Kulkarni R.K., Pani K.C., Neuman C., Leonard F., Polylactic Acid for Surgical Implants, *Arch. Surg.*, **93(5)**: 839-843 (1966).

[6] Aziz T., Ullah A., Ali A., Shabeer M., Shah M.N., Haq F., Iqbal M., Ullah R., Khan F.U., Manufactures of Bio-Degradable and Bio-Based Polymers for Bio-Materials in the Pharmaceutical Field, *J. Appl. Polym. Sci*., **139(29)**: 52624-52634 (2022).

[7] Janik H., Marzec M., A Review: Fabrication of Porous Polyurethane Scaffolds, *Mater. Sci. Eng: C.*, **48**: 586–591 (2015).

[8] Samatya Yilmaz S., Aytac A., Poly (Lactic Acid)/Polyurethane Blend Electrospun Fibers: Structural, Thermal, Mechanical and Surface Properties, *Iranian Polym. J.*, **30**: 873-883 (2021).

[9] Sun B., Duan B., Yuan X., Preparation of Core/Shell PVP/PLA Ultrafine Fibers by Coaxial Electrospinning, *J. Appl. Polym. Sci.*, **102(1)**: 39–45 (2006).

[10] Unnithan A.R., Sasikala A.R.K., Murugesan P., Gurusamy M., Wu D., Park C.H., Kim C.S Electrospun polyurethane-Dextran Nanofiber Mats Loaded with Estradiol for Post-Menopausal Wound Dressing, *Int. J. Biol. Macromol.* **77**: 1-8 (2015).

[11] Dehcheshmeh M.A., Fathi M., Production of Core-Shell Nanofibers from Zein and Tragacanth for Encapsulation of Saffron Extract, *Int. J. Biol. Macromol.*, **122**: 272–279 (2018).

[12] Alippilakkottea S., Kumar S., Sreejith L., Fabrication of PLA/Ag Nanofibers by Green Synthesis Method Using Momordica Charantia Fruit Extract for Wound Dressing Applications, *Collo. Surf. A: Phys. Eng. Asp.*, **529**: 771-782 (2017).

[13] Lakshman L.R., Shalumon K., Nair S.V., Jayakumar R., Preparation of Silver Nanoparticles Incorporated Electrospun Polyurethane Nano-Fibrous Mat for Wound Dressing, *J. Macromol. Sci. Part A: Pure Appl. Chem.*, **47(10)**: 1012–1018 (2010).

[14] Nguyen T.T.T., Chung O.H., Park J.S., Coaxial Electrospun Poly(Lactic Acid)/Chitosan (Core/Shell) Composite Nanofibers and their Antibacterial Activity, *Carbohydr. Polym.*, **86(4)**: 1799–1806 (2011).

[15] Hajikhani M., Djomeh Z.E., Askari G., Fabrication and Characterization of Mucoadhesive Bioplastic Patch via Coaxial Polylactic Acid (PLA) Based Electrospun Nanofibers with Antimicrobial and Wound Healing Application, *Inter. J. Bio. Macromol.*, **172**: 143–153 (2021).

[16] Zeytuncu B., Morcali M.H., Fabrication and Characterization of Antibacterial Polyurethane Acrylate-Based Materials, *Mat. Res.*, **18(4)**: 867-872 (2015).

[17] Hsu S., Tseng H.J, Lin Y.C., The Biocompatibility and Antibacterial Properties of Waterborne Polyurethane-Silver Nanocomposites, *Biomaterials*., **31(26)**: 6796-6808 (2010).

[18] Lan X., Liu Y., Wang Y., Tian F., Miao X., Wang H., Tang Y., Coaxial Electrospun PVA/PCL Nanofibers with Dual Release of Tea Polyphenols and ε-POLY (L-Lysine) as Antioxidant and Antibacterial Wound Dressing Materials, *Inter. J. Pharm.*, **601**: 120525-120535 (2021).

[19] Guo Y., An X., Fan Z., Aramid Nanofibers Reinforced Polyvinyl Alcohol/Tannic Acid Hydrogel with Improved Mechanical and Antibacterial Properties for Potential Application as Wound Dressing, *J. Mech. Behav. Biomed. Mater.*, **118**: 104452-104466 (2021).

[20] Wu J.Y., Ooi C.W., Song C.P., Wang C.Y., Liu B.L., Lin G.Y, Chiu C.Y., Chang Y.K., Antibacterial Efficacy of Quaternized Chitosan/Poly (Vinyl Alcohol) Nanofiber Membrane Crosslinked with Blocked Diisocyanate, *Carbohydr. Polym.*, **262**: 117910-117921 (2021).

[21] Ramakrishna S., Fujihara K., Teo W.E., Yong T., Ma Z., Ramaseshan R., Electrospun Nanofibers: Solving Global Issues, *Mater. Today.*, **9(3)**: 40-50 (2006).

[22] Khwanmuang P., Naparswad C., Archakunakorn S., Waicharoen C., Chitichotpanya C., Optimization of in Situ Synthesis of Ag/PU Nanocomposites Using Response Surface Methodology for Self-Disinfecting Coatings, *Prog. Org. Coat.*, **110**: 104-113 (2017).

[23] Fukushima J., Yasuda K., Teratani H., Nishizaki S., Settling Behavior of Fillers in Thermosetting Epoxy Casting Resins During Cure, *J. Appl. Polym. Sci.*, **22(6)**: 1701-1714 (1978).

[24] Jia W., Tchoudakov R., Joseph R., Narkis M., Siegmann A., The Conductivity Behavior of Multi-Component Epoxy, Metal Particle, Carbon Black, Carbon Fibril Composites, *J. Appl. Polym. Sci.*, **85(8)**: 1706-1713 (2002).

[25] Li J., Peng W.J., Fu Z.J., Tang X.H., Wu H., Guo S., Wang M., Achieving High Electrical Conductivity and Excellent Electromagnetic Interference Shielding in Poly(Lactic Acid)/Silver Nanocomposites by Constructing Large-Area Silver Nanoplates in Polymer Matrix, *Composites*, **171**: 204-213 (2019).

[26] Sayyar M., Soroushian P., Abdol N., Staggemeier K., Bakker M.G.,Balachandra A.M., High Performance Pseudoelastic Metal Nanowire Reinforced Elastomeric Composite, *Ind. Eng. Chem. Res.*, **53(34)**: 13329-13339 (2014).

[27] Pradhan K.C., Nayak P.L., Synthesis and Characterization of Polyurethane Nanocomposite from Castor Oil-Hexamethylene Diisocyanate (HMDI), *Adv. Appl. Sci. Res.*, **3(5)**: 3045-3052 (2012).

[28] Feng F., Ye L., Morphologies and Mechanical Properties of Polylactide/Thermoplastic Polyurethane Elastomer Blends, *J. Appl. Polym. Sci.*, **119(5)**: 2778-2783 (2010).

[29] Erbil H.Y., Demirel A.L., Avci Y., Mert O., Erbil H.Y., Demirel A.L., Avci Y., Mert O., Transformation of a Simple Plastic into a Superhydrophobic Surface, *Science*, **299(5611)**: 1377-1380 (2003).

[30] Krishna K., Harisha K.S., Neelakandan R., Fabrication and Conductivity Study of Silver Nanoparticles Loaded Polyvinyl Alcohol (PVA-AgNPs) Nanofibers, *Mater. Today: Proceed.*, **42(2)**: 515-520 (2021).

[31] Chernousova S., Epple M., Silver as Antibacterial Agent: Ion, Nanoparticle, and Metal, *Chem. Int. Ed.*, **52(6)**: 1636–1653 (2013).

[32] Sun Z., Fan C., Tang X., Zhao J., Song Y., Shao Z., Xu L., Characterization and Antibacterial Properties of Porous Fibers Containing Silver Ions, *Appl. Surf. Sci.*, **387**: 828-838 (2016).

[33] Li R., Cheng Z., Yu X., Wang S., Han Z., Kang L., Preparation of Antibacterial PCL/PVP-AgNP Janus Nanofibers by Uniaxial Electrospinning, *Mater. Lett.*, **254**: 206-209 (2019).

[34] Momeni M., Asadi, S., Shanbedi M., Antimicrobial Effect of Silver Nanoparticles Synthesized with Bougainvillea Glabra Extract on Staphylococcus Aureus and Escherichia Coli, *Iran. J. Chem. Chem. Eng. (IJCCE),* **40(2)**: 395-405 (2021).

[35] Ghorbani M., Ehsani Amoli A., Soleimani Lashkenari M., Polypyrrole/Silver Nanocomposite: Synthesis, Characterization and Antibacterial Activity, *Iran. J. Chem. Chem. Eng.n(IJCCE),* **38(3)**: 1-7 (2019).

[36] Zhang S., Ye J., Sun Y., Kang J., Liu J., Wang Y., Li Y., Zhang L., Ning G., Electrospun Fibrous Mat Based on Silver (I) Metal-Organic Frameworks-Polylactic Acid for Bacterial Killing and Antibiotic-Free Wound Dressing, *Chem. Eng. J.*, **390**: 124523-124533, (2020).

[37] Feng Q.L., Wu J., Chen G.Q., Cui F.Z., Kim T.N., Kim J.O., A Mechanistic Study of the Antibacterial Effect of Silver İons on Escherichia Coli and Staphylococcus Aureus, *J. Biom. Mater. Res.*, **52(4)**: 662-668 (2020).

[38] Movahedi M., Asefnejad A., Rafienia M., Khorasani M.T., Potential of Novel Electrospun Core-Shell Structured Polyurethane/Starch (Hyaluronic Acid) Nanofibers for Skin Tissue Engineering: In Vitro and in Vivo Evaluation, *Int. J. Biol. Macromol.*, **146**: 627-637 (2020).